

Study of IMF and its North-South Component (B_z) When $DST \leq -100nT$ during Geomagnetic Storm

Megha Agari, L. P. Verma

Department of Physics, Govt Degree College, Shitlakhet-263678, Almora, Uttarakhand, India, e-mail:
meghamishti1996@gmail.com

ABSTRACT

The interplanetary magnetic field, its east-west component (B_y), and its north-south component (B_z) fluctuate within solar activity and play a key role in the interaction of the solar wind with Earth's magnetosphere. In this manuscript, daily averaged data spanning the initial decade (from 1 January 2014 to 5 May 2024) were employed to establish the criteria $-130nT \leq Dst \leq -100nT$. A significant, moderate, and weak correlation between geomagnetic storms and the interplanetary magnetic field (IMF), B_y , and B_z has been identified. For instance, the IMF exhibits an anti-correlation coefficient of -0.7 in the years 2023 and 2015. Additionally, B_y and B_z demonstrate a robust correlation coefficient of +0.7 in the year 2018.

Keywords. Geomagnetic index, interplanetary magnetic field, magnetosphere.

1. Introduction

The predominant factor contributing to geomagnetic storms is the presence of solar wind structures that are associated with a pronounced southward interplanetary magnetic field (IMF), which interact with the Earth's magnetic field and facilitate the transfer of solar wind energy into the Earth's magnetosphere. Geomagnetic storms may arise from two distinct types of IMF structures: high-velocity wind streams and coronal mass ejections (CMEs) (Gonzalez et al., 1999). The current systems within the magnetosphere-ionosphere are significantly affected by the interplanetary magnetic field as elucidated in the literature (e.g., Juusola et al., 2014; Huang et al., 2017; Laundal et al., 2018; Milan et al., 2017; Reistad et al., 2014; Smith et al., 2017). Previous examinations of the Interplanetary Magnetic Field (IMF) and its components in geocentric solar magnetospheric (GSM) coordinates indicate that the IMF B_z (north-south component) delineates the comprehensive convection pattern of the plasma, which is concomitant with the high-latitude ionosphere in both the northern and southern hemispheres. Specifically, this encompasses two vortex cells alongside an anti-sunward flow over the polar cap, in conjunction with a sunward return flow traversing the lower latitudes during both the morning and evening sectors (convection pattern of two-cell) under conditions of entirely southward IMF. Conversely, in the case of a northward IMF, it is observed that two additional cells with opposing vorticity (convection pattern of four cells) may persist within the central polar cap. These cells are identified as being significantly distorted in the direction of either the dawn or dusk sector, contingent upon the polarity of the dawn-dusk IMF B_y (Heppner & Maynard, 1987).

The contribution of IMF B_x in reconnection processes as well as the evolution of ionospheric plasma flow samples, has not been as broadly considered; for example, the high-latitude convection statistical models are generally prepared concerning the IMF B_x and B_y . Nevertheless, the confirmation has revealed implying at the potential significance of IMF B_x to lobe reconnection processes (e.g., Förster & Haaland, 2015; Taguchi & Hoffman, 1995). It has been extensively established over an extended duration that the interplanetary magnetic

field's B_Y component serves as a pivotal element in the dynamics between solar wind and the magnetosphere; for illustrative purposes, one may reference the convection patterns observed in auroral regions and polar caps (Cowley et al., 1991; Heppner & Maynard, 1987; Ruohoniemi & Greenwald, 1996, 2005; Thomas & Shepherd, 2018). Within the confines of the magnetosphere, the y component exhibits a positive correlation with the interplanetary magnetic field component across both open and closed magnetic field lines (e.g., Fairfield, 1979; Cowley and Hughes, 1983; Lui, 1984; Kaymaz et al., 1994; Wing et al., 1995; Petrukovich et al., 2005; Case et al., 2021).

2. Data Analysis

The daily averaged data downloaded from (omniweb.gsfc.nasa.gov/form/dx1.html) spanning a decade (from 1 January 2014 to 5 May 2024) were meticulously analyzed within the context of the GSM system. This investigation delves into the annual fluctuations of the Interplanetary Magnetic Field (IMF) and its B_z component about geomagnetic activity, utilizing the specified criteria of $-130\text{nT} \leq \text{Dst} \leq -100\text{nT}$ for the initial ten years of data. Subsequently, a superposed epoch analysis has been employed for both investigations, taking into account the $\pm 1, \pm 2, \pm 3, \pm 4, \dots, \pm 18$ events surrounding the designated zero day. Correlation coefficients have been observed regarding the annual variations among various parameters, including IMF, B_Y , B_Z , and the Dst-index. The correlation coefficient is constrained within the range of -1 to $+1$, wherein the extremities denote the maximum correlation, while a value of zero indicates the absence of correlation (Silwal et al., 2021; Ratner, 2009). In the analysis of a decade's worth of data, we observe noteworthy findings for the years 2015, 2018, and 2023.

3. Study of the IMF B_z magnitude concerning geomagnetic activity

At the minimum value of Dst, the maximum inclination in magnitude of the interplanetary magnetic field (IMF) has been observed to occur on the zero-day for the years 2015, 2018, and 2023, particularly in 2023 strong correlation of -0.7 has been found between the Dst and the IMF, exhibiting variations up to its highest magnitude, which is recorded to lie within the range of 18nT to 20nT . A moderate relationship has been found of -0.6 between Dst and IMF as well as in the period spanning from $+5$ to $+10$ days the magnitude of the IMF decreases to levels below 4nT in 2015, whereas in 2018, the lowest magnitude is observed to drop below 3nT during the (15-18) days preceding the event and moderate correlation of -0.6 observed.

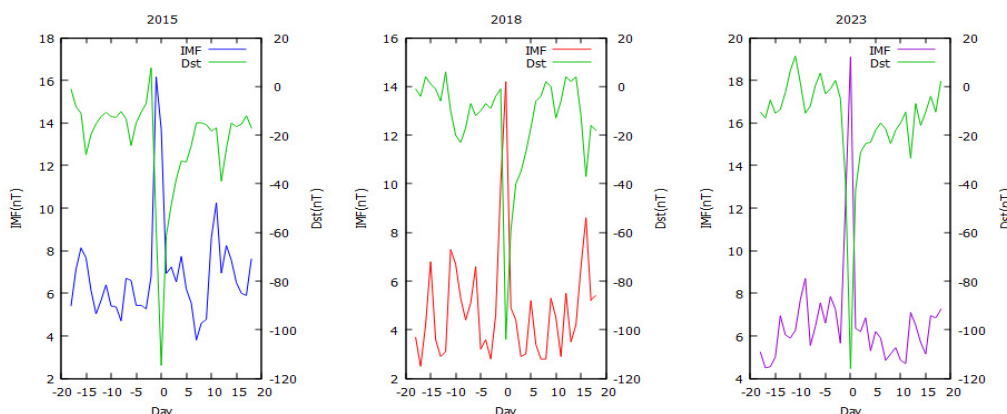


Figure 1. The following time series representation illustrates the ± 18 -day period surrounding the event concerning the daily mean values of the interplanetary magnetic field alongside the Dst index for 2015, 2018, and 2023.

For the energy transfer in the terrestrial magnetosphere from the solar wind, the major factor is the orientation of the interplanetary magnetic field (Tenfjord & Østgaard, 2013). IMF B_z powerfully controls the transfer of energy because it greatly determines whether the magnetic field of Earth is antiparallel or not.

In the examination of the oscillations of B_z , we analyze the temporal interval that precedes the event by 18 days, during which B_z commences to display fluctuations at magnitudes below zero. As indicated by prior research, the intensity of geomagnetic storms exhibits a significant dependency on the southward component B_z (Rathore et al., 2014); however, this study reveals that such a result was exclusively observed in the year 2018, while a moderate dependency was noted in the years 2015 and 2023. In the year 2018, the lowest recorded Dst, along with the most significant negative B_z peak, was documented on the initial day; in contrast, the highest peak occurred within the range of +10 to +15 days. In the year 2015, the minimum declination in the Interplanetary Magnetic Field (IMF) was observed at the maximum inclination in the Disturbance Storm Time (Dst) index before a timeframe of 0 to 5 days preceding the event. Moreover, for the year 2023, the lowest and highest peaks of IMF magnitude were identified for the interval of 0 to 5 days before the event (see Figure 2).

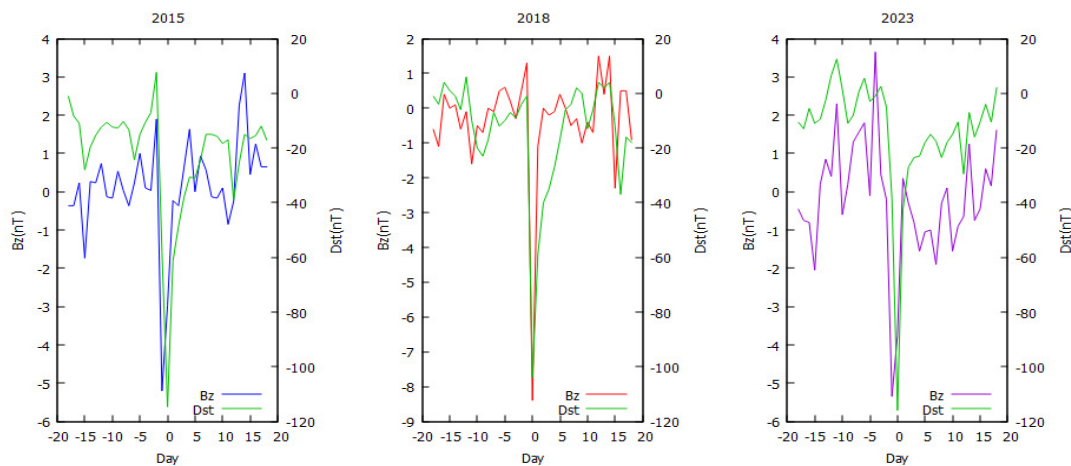


Figure 2. The outcomes of the superposed epoch analysis extend from -18 to +18 days in relation to the day of the geomagnetic storm occurrence (designated as zero epoch). The illustration delineates the fluctuation of the average values of Dst and the mean values of IMF B_z for the years 2015, 2018, and 2023.

Within the magnetosphere, the solar wind kinetic energy can be transformed into magnetic energy during magnetic reconnection. When the IMF B_y is strong, (Wilcox & Ness, 1965), frequently magnetic tension deflects the consequential flow of plasma variably on newly magnetic open field lines in both hemispheres, and leads a notable asymmetries in the magnetosphere (Tenfjord et al., 2015) explicit in auroral intensity (Newell et al., 2004; Shue et al., 2001), global convection patterns (Haaland et al., 2007; Heppner & Maynard, 1987; Pettigrew et al., 2010) and currents (Anderson et al., 2008; Green et al., 2009; Laundal, Gjerlov, et al., 2016). For the year 2018, during periods of minimal disturbance represented by Dst (zero-day), the highest peak variations in the magnitude of B_y have been observed, with values oscillating between 5nT and 6nT. And the lowest peak has been found between the magnitude -3nT and -4nT for 0-5 days preceding the event. The maximum recorded inclination in the magnitude of B_y occurred on the +18 day in 2015, coinciding with the lowest declination observed between the 10-15 day interval following the event at a low Dst magnitude. In the year 2023, at minimal Dst levels, the magnitude of B_y fluctuates to -10nT on zero day, while the maximum inclination has been detected five days before the event, during which its magnitude reaches 4nT at a positive Dst magnitude.

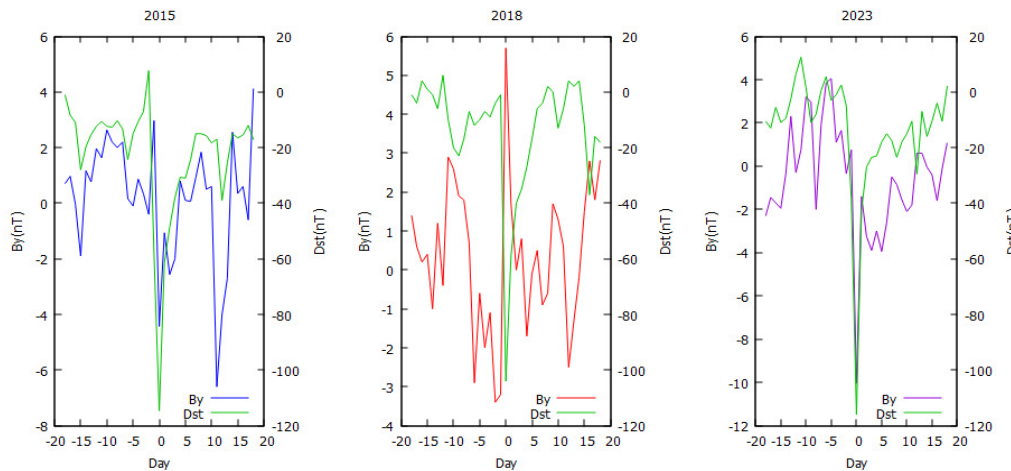


Figure 3. Superposed epoch analysis of the magnetic field component IMF B_Y concerning geomagnetic activity for the temporal periods of -18 and +18 days encircling a specific event, for the years 2015, 2018, and 2023.

4. Conclusion

The fluctuations of the Interplanetary Magnetic Field (IMF) and its east-west component (B_Y) alongside its north-south component (B_Z) as delineated in this research, IMF reveal a significant inverse correlation (-0.7) with the Dst index for the years 2015 and 2023, as well as a correlation of -0.6 for the year 2018. The peak inclination was observed in 2015 within a timeframe of 0-3 days before the event, during which the magnitude of the IMF exceeded 16nT. Furthermore, the B_Z component demonstrates a robust positive correlation (+0.7) with the Dst index in 2018, while also showcasing moderate correlations of +0.5 in 2015 and +0.6 in 2023. The magnitude of B_Z attains its maximum inclination within the range of 18nT to 20nT, indicating that the corresponding level of geomagnetic activity remains low (characterized by minimum Dst values). The east-west component demonstrated a robust correlation of +0.7 in the year 2023, while presenting a moderate correlation of -0.5 in 2018 and a weak correlation of +0.4 in 2015. The peak inclination for this phenomenon has been identified on the initial day for this magnitude of B_Y , reaching up to 14nT.

| | 2015 | 2018 | 2023 |
|------------|------|------|------|
| IMF, nT | -0.7 | -0.6 | -0.7 |
| B_Y , nT | 0.4 | -0.5 | 0.7 |
| B_Z , nT | 0.5 | 0.7 | 0.6 |

Table 1. The outcomes derived from the superposed epoch analysis spanning from +18 to +18 days for the annual investigation of solar cycle 25.

Acknowledgment

I would like to express my gratitude to the OMNI (Operating Mission as a Node on the Internet) database of NASA (National Aeronautics and Space Administration).

References

- Anderson, B. J., Korth, H., Waters, C. L., Green, D. L., & Stauning, P. (2008). Statistical Birkeland current distributions from magnetic field observations by the iridium constellation. *Annals of Geophysics*, **26**, 671–687.
- Case, N. A., Hartley, D. P., Grocott, A., Miyoshi, Y., Matsuoka, A., Imajo, S., et al. (2021). Inner magnetospheric response to the interplanetary magnetic field by component: Van allen probes and ARASE observations. *JGR. Space Phys.* 126, e2020JA028765. doi:10.1029/2020JA028765
- Cowley, S. W.H., and Hughes, W.J.(1983).Observation of an IMF sector effect in the Y magnetic field component at geostationary orbit. *Planet. Space Sci.* 31, 73–90. doi:10.1016/0032-0633(83)90032-6
- Cowley, S. W. H., Morelli, J. P., & Lockwood, M. (1991). Dependence of convective flows and particle precipitation in the high-latitude dayside ionosphere on the x and y components of the interplanetary magnetic field. *Journal of Geophysical Research*, 96(A4), 5557–5564.
<https://doi.org/10.1029/90ja02063>
- Fairfield, D. H. (1979). On the average configuration of the geomagnetic tail. *J. Geophys. Res.* 84, 1950–1958. doi:10.1029/JA084iA05p01950
- Förster, M., & Haaland, S. (2015). Interhemispheric differences in ionospheric convection: Cluster EDI observations revisited. *Journal of Geophysical Research: Space Physics*, **120**, 5805–5823. <https://doi.org/10.1002/2014JA020774>
- Green, D. L., Waters, C. L., Anderson, B. J., & Korth, H. (2009). Seasonal and interplanetary magnetic field dependence of the field-aligned currents for both Northern and Southern Hemispheres. *Annals of Geophysics*, **27**, 1701–1715. <https://doi.org/10.5194/angeo-27-1701-2009>
- Haaland, S. E., Paschmann, G., Förster, M., Quinn, J. M., Torbert, R. B., McIlwain, C. E., et al. (2007). High-latitude plasma convection from Cluster EDI measurements: Method and IMF-dependence. *Annals of Geophysics*, **25**, 239–253. <https://doi.org/10.5194/angeo-25-239-2007>
- Heppner, J. P., & Maynard, N. C. (1987). Empirical high-latitude electric field models. *Journal of Geophysical Research*, **92**, 4467–4489. <https://doi.org/10.1029/JA092iA05p0446>
- Huang, Tao., Lühr, H., & Wang, H. (2017). Global characteristics of auroral Hall currents derived from the Swarm constellation: dependences on season and IMF orientation. *Annales Geophysicae*, 35(6), 1249–1268. <https://doi.org/10.5194/angeo-35-1249-2017>
- Juusola, L., Milan, E. S., Lester, M., Grocott, A., & Imber, M. S. (2014). Interplanetary magnetic field control of the ionospheric field-aligned current and convection distributions. *Journal of Geophysical Research: Space Physics*, 119(4), 3130–3149. <https://doi.org/10.1002/2013ja019455>
- Kaymaz, Z., Siscoe, G. L., Luhmann, J. G., Lepping, R. P., and Russell, C. T. (1994). Interplanetary magnetic field control of magnetotail magnetic field geometry: IMP 8 observations. *J. Geophys. Res.* 99, 11113–11126. doi:10.1029/94JA00300
- Laundal, K. M., Gjerloev, J. W., Ostgaard, N., Reistad, J. P., Haaland, S. E., Snekvik, K., et al. (2016). The impact of sunlight on high-latitude equivalent currents. *Journal of Geophysical Research*, **121**, 2715–2726. <https://doi.org/10.1002/2015JA022236>
- Laundal, K. M., Finlay, C. C., Olsen, N., & Reistad, J. P. (2018). Solar wind and seasonal influence on ionospheric currents from Swarm and CHAMP measurements. *Journal of Geophysical Research: Space Physics*, 123(5), 4402–4429. <https://doi.org/10.1029/2018ja025387>
- Lui, A. T. Y. (1984). “Characteristics of the cross-tail current in the Earth’s magnetotail,” in *Magnetospheric currents*. Editor T. A. Potemra (American Geophysical Union), 28, 158–170. doi:10.1029/GM028p0158
- Milan, S. E., Clausen, L. B. N., Coxon, J. C., Carter, J. A., Walach, M. T., Laundal, K., et al. (2017). Overview of solar wind–magnetosphere–ionosphere–atmosphere coupling and the generation of magnetospheric currents. *Space Science Reviews*, 206(1–4), 547–573. <https://doi.org/10.1007/s11214-017-0333-0>

(Newell et al., 2004; Shue et al., 2001), global convection patterns (Haaland et al., 2007; Heppner & Maynard, 1987; Pettigrew et al., 2010) and currents (Anderson et al., 2008; Green et al., 2009; Laundal, Gjerlov, et al., 2016). <https://doi.org/10.1002/2017JA024864>

Petrukovich, A. A., Baumjohann, W., Nakamura, R., Runov, A., and Balogh, A. (2005). Cluster vision of the magnetotail current sheet on a macroscale. *J. Geophys. Res.* 110, A06204. doi:10.1029/2004JA010825

Pettigrew, E. D., Shepherd, S. G., & Ruohoniemi, J. M. (2010). Climatological patterns of high-latitude convection in the Northern and Southern hemispheres: Dipole tilt dependencies and interhemispheric comparison. *Journal of Geophysical Research*, **115**, A07305. <https://doi.org/10.1029/2009JA014956>

Rathore, B.S., Gupta, D. C., and Parashar K. K.K., *Int. J. Geosci.* 05, 1602 (2014). <http://dx.doi.org/10.4236/ijg.2014.513131>

Ratner, B. The correlation coefficient: Its values range between +1/−1, or do they?. *J Target Meas Anal Mark* **17**, 139–142 (2009). <https://doi.org/10.1057/jt.2009.5>

Reistad, J. P., Østgaard, N., Laundal, K. M., Haaland, S., Tenfjord, P., Snekvik, K., et al. (2014). Intensity asymmetries in the dusk sector of the poleward auroral oval due to IMF B_x. *Journal of Geophysical Research: Space Physics*, 119(12), 9497–9507. <https://doi.org/10.1002/2014JA020216>

Ruohoniemi, J. M., & Greenwald, R. A. (2005). Dependencies of high-latitude plasma convection: Consideration of interplanetary magnetic field, seasonal, and universal time factors in statistical patterns. *Journal of Geophysical Research*, 110(A9). <https://doi.org/10.1029/2004ja010815>

Smith, A. R. A., Beggan, C. D., Macmillan, S., & Whaler, K. A. (2017). Climatology of the auroral electrojets derived from the along-track gradient of magnetic field intensity measured by pogo, magsat, Champ, and swarm. *Space Weather*, 15(10), 1257–1269. <https://doi.org/10.1002/2017sw001675>

Shue, J. H., Newell, P.T., Liou, C., Meng, C. I. Influence of interplanetary magnetic field on global auroral patterns. *Journal of Geographical Research: Space Physics* <https://doi.org/10.1029/2000JA003010>

Taguchi, S., & Hoffman, R. A. (1995). B_x control of polar cap potential for northward interplanetary magnetic field. *Journal of Geophysical Research*, **100**, 19,313–19,320. <https://doi.org/10.1029/95JA01085>

Thomas, E. G., & Shepherd, S. G. (2018). Statistical patterns of ionospheric convection derived from mid-latitude, high-latitude, and polar Super-DARN HF radar observations. *Journal of Geophysical Research*, 123(4), 3196–3216. <https://doi.org/10.1002/2018ja025280>

Tenfjord, P., & Østgaard, N. (2013). Energy transfer and flow in the solar wind-magnetosphere-ionosphere system: A new coupling function. *Journal of Geophysical Research*, **118**, 5659–5672. <https://doi.org/10.1002/jgra.50545>

Tenfjord, P., Østgaard, N., Snekvik, K., Laundal, K. M., Reistad, J. P., Haaland, S., & Milan, S. (2015). How the IMF B_y induces a B_y component in the closed magnetosphere and how it leads to asymmetric currents and convection patterns in the two hemispheres. *Journal of Geophysical Research: Space Physics*, **120**, 9368–9384. <https://doi.org/10.1002/2015JA02157>

Wilcox, J. M., & Ness, N. F. (1965). Quasi-stationary corotating structure in the interplanetary medium. *Journal of Geophysical Research*, **70**(23), 5793–5805. <https://doi.org/10.1029/JZ070i023p05793>